Available online at www.sciencedirect.com
ScienceDirect
Biochimica et Biophysica Acta 1768 (2007) 218–227
Biochimica et Biophysica Acta
BBA
www.elsevier.com/locate/bbamem

Structure and localization of an essential transmembrane segment of the proton translocation channel of yeast H^+-V-ATPase

Afonso M.S. Duarte [a], Cor J.A.M. Wolfs [a], Nico A.J. van Nuland [d,1], Michael A. Harrison [c], John B.C. Findlay [c], Carlo P.M. van Mierlo [b], Marcus A. Hemminga [a,*]

[a] *Laboratory of Biophysics, Wageningen University, Dreijenlaan 3, 6703 HA Wageningen, The Netherlands*
[b] *Laboratory of Biochemistry, Wageningen University, The Netherlands*
[c] *School of Biochemistry and Molecular Biology, University of Leeds, The Netherlands*
[d] *Department of NMR Spectroscopy, Bijvoet Centre for Biomolecular Research, University of Utrecht, The Netherlands*

Received 5 April 2006; received in revised form 12 July 2006; accepted 28 July 2006
Available online 2 August 2006

Abstract

Vacuolar (H^+)-ATPase (V-ATPase) is a proton pump present in several compartments of eukaryotic cells to regulate physiological processes. From biochemical studies it is known that the interaction between arginine 735 present in the seventh transmembrane (TM7) segment from subunit *a* and specific glutamic acid residues in the subunit *c* assembly plays an essential role in proton translocation. To provide more detailed structural information about this protein domain, a peptide resembling TM7 (denoted peptide MTM7) from *Saccharomyces cerevisiae* (yeast) V-ATPase was synthesized and dissolved in two membrane-mimicking solvents: DMSO and SDS. For the first time the secondary structure of the putative TM7 segment from subunit *a* is obtained by the combined use of CD and NMR spectroscopy. SDS micelles reveal an α-helical conformation for peptide MTM7 and in DMSO three α-helical regions are identified by 2D ^{1}H-NMR. Based on these conformational findings a new structural model is proposed for the putative TM7 in its natural environment. It is composed of 32 amino acid residues that span the membrane in an α-helical conformation. It starts at the cytoplasmic side at residue T719 and ends at the luminal side at residue W751. Both the luminal and cytoplasmatic regions of TM7 are stabilized by the neighboring hydrophobic transmembrane segments of subunit *a* and the subunit *c* assembly from V-ATPase.

Keywords: NMR; CD; V-ATPase subunit *a*; Peptide; Protein conformation

1. Introduction

Vacuolar (H^+)-ATPase (V-ATPase) is a large multi-protein membrane-bound enzymatic complex present in almost all types of eukaryotic cells [1–3]. It can be found both in the intracellular and plasma membrane. It plays an important role in endocytosis, intracellular targeting, in protein processing and degradation. In plasma membranes the protein is involved in renal acidification, pH homeostasis, and in bone resorption [3,4]. The bone resorption process occurs in the membranes of osteoclast cells and is an important step in the maintenance of bone tissue [1,5]. The deregulation of osteoclasts can originate a higher bone removal provoking osteoporosis. The drugs available at the moment to reduce bone loss only have a temporary effect, so new therapies are needed that work longer

Abbreviations: CD, Circular Dichroism; CSI, Chemical shift index; DMSO, Dimethylsulfoxide; DSS, Sodium 2,2-dimethyl-2-silapentane-5-sulfonate; DTT, Dithiothreitol; HMBC, Heteronuclear multiple bond correlation; HSQC, Heteronuclear single quantum coherence; MTM7, Peptide mimicking the seventh transmembrane segment of subunit *a* from V-ATPase; NMR, Nuclear magnetic resonance; NOESY, Nuclear Overhauser enhanced spectroscopy; SDS, Sodium dodecyl sulfate; TM, Transmembrane; TOCSY, Total correlation spectroscopy; V-ATPase, Vacuolar proton-translocating adenosine triphosphatase; Vma, Vacuolar membrane ATPase encoding genes; Vph, Vacuolar acidification encoding genes

* Corresponding author. Tel.: +31 317482635; fax: +31 317 482 725.
E-mail address: marcus.hemminga@wur.nl (M.A. Hemminga).
URL: http://ntmf.mf.wau.nl/hemminga/ (M.A. Hemminga).
[1] Present address: Departamento de Química Física y Instituto de Biotecnología, Facultad de Ciencias, Universidad de Granada, Campus Fuentenueva s/n, 18071 Granada, Spain.

0005-2736/$ - see front matter © 2006 Elsevier B.V. All rights reserved.
doi:10.1016/j.bbamem.2006.07.014

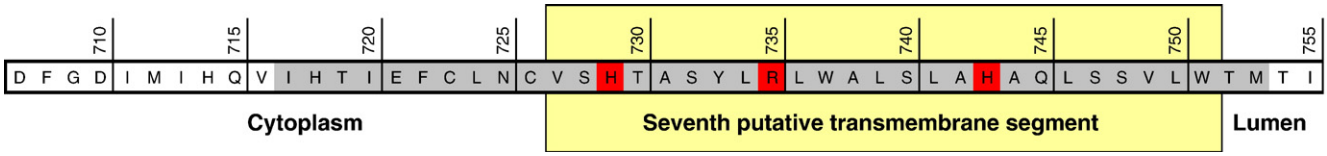

Fig. 1. Partial sequence of subunit *a* from yeast V-ATPase, including the putative TM7 segment [3] (yellow box). Peptide MTM7 (shown in gray) includes residues I717 up to M753. The functional amino acid residues in TM7 (H728, R735 and H743) are indicated in red. The numbering of the residues in peptide MTM7 is according to the numbering of the entire subunit *a* [3].

and are more specific. The discovery of new inhibitors specific for V-ATPase is required to allow the control of bone removal. The know-how to do so has been hampered due to the absence of a high-resolution structure of the V-ATPase system. This information together with dynamical studies of the system can help to indicate targeting points that can be used to control V-ATPase in human osteoclast cells.

The V-ATPase from yeast is the most studied member of the V-ATPase family of enzymes due to the relative ease of its biochemical manipulation. Via ATP hydrolysis, V-ATPase translocates protons across the membrane against the electrochemical potential. ATP hydrolysis occurs in subunits A and B in the cytoplasmic domain (V_1), while proton translocation is achieved by the transmembrane subunits in the membrane domain (V_O). The V_O domain is composed of four subunits: *a*, *c*, *c′* and *c″*. The subunit *c* ensemble (*c* (Vma3p), *c′* (Vma11p) and *c″* (Vma16p)) is part of the rotary motor, while subunit *a* (Vph1p or Stv1p) [6] forms the stator.

One of the approaches to discover a way to control the function of the enzyme aims at finding compounds that interact with the transmembrane subunits involved in proton translocation. To enhance these studies high-resolution structures of the transmembrane region are needed. The only high-resolution structure of the V_O domain known at this moment is from the rotor of the gram-positive bacterium *Enterococcus hirae* [7]. Regarding subunit *a* only a low-resolution structure is available together with biochemical information [8]. Disulphide-mediated cross-linking and labelling experiments with subunit *a* suggest that it is composed of nine putative transmembrane helices and that it has a cytoplasmic domain of 400 residues [9]. The hydrophilic amino terminal part of subunit *a* is located in the cytoplasm and its hydrophilic carboxyl terminal part is located in the lumen [9,10]. It has also been reported that residue R735 in the seventh putative transmembrane segment (TM7) of subunit *a* plays a vital role in proton translocation [10]. Mutation of R735 induces a total inhibition of proton translocation, while mutations in other sections of the membrane-spanning region have less inhibitory effects.

Subunits *c*, *c′* and *c″* of the rotor of yeast V-ATPase are composed of four transmembrane segments and subunit *c″* contains in addition a fifth cytoplasmic segment [3]. The glutamic acid residues present in the fourth putative transmembrane segment of *c* and *c′*, and in the second transmembrane putative segment of *c″*, are known to be essential for the proton translocation capacity of the rotor [3,9,11].

In the most recent model that describes proton translocation by V-ATPase an interaction between R735 (on TM7 of subunit *a*) and the glutamic acids from the subunit *c* ensemble (E137 on TM4 of subunit *c*, E145 on TM4 of subunit *c′*, and E108 on TM2 of subunit *c″*) is essential [10,12]. Proton translocation happens via the integration of the proton in the subunit *c* assembly. Subsequently the rotation of the motor delivers the proton into the lumen [9].

In our work, we assume that the conformation of a putative transmembrane peptide in a membrane-mimicking solvent is related to the conformation in its native environment. It is obvious that in this case interactions with the surrounding transmembrane segments are lacking. However, the usefulness and practicability of this approach is supported by several structural studies on different membrane proteins: Ca^{2+}–ATPase [13], F_O–F_1–ATPase [14], potassium ion channel [15], divalent metal transporter protein [16], bacteriorhodopsin [17,18], rhodopsin [19], thrombomodulin [20], and G-protein coupled receptor [21]. It is interesting to note that in some of these studies the secondary structures obtained for the isolated transmembrane segments were indeed confirmed when the structure of the complete protein was published [17,19,22]. Thus, the structure of an isolated putative transmembrane segment contains information on the natural conformational propensity of the complete transmembrane proteic domain.

In this paper we report the conformational properties of the putative seventh transmembrane segment (TM7) of subunit *a* (Vph1) from the yeast *Saccharomyces cerevisiae* V-ATPase. This transmembrane segment contains the essential R735. A peptide that mimics the putative TM7 segment (denoted peptide MTM7) is designed and synthesized (Fig. 1). Circular dichroism spectroscopy (CD) reveals the secondary structure of peptide MTM7 in SDS micelles and is used to characterize its thermal stability. Two-dimensional (2D) ^{1}H-NMR spectroscopy is applied to probe the conformational properties of the peptide in DMSO. These results provide information about the conformation and position of the putative seventh transmembrane segment within the native hydrophobic environment of V-ATPase.

2. Materials and methods

2.1. Peptide design and synthesis

Based on the predicted localization of the seventh putative transmembrane segment (TM7) from subunit *a* from yeast [3], a 37-residue peptide (MTM7) was designed (Fig. 1). MTM7 includes the putative membrane-spanning section V727 to M753 in which the activity-related amino acid residues (H729, R735 and H743) are located [3]. Residue R735 was placed in the center of the peptide similar to as what would be expected for the corresponding membrane segment in its natural environment [3]. The peptide also includes part of the cytoplasmic and luminal putative turns. Throughout the paper the numbering of the amino acid residues in peptide MTM7 will be the same as is used for the native subunit *a* (Fig. 1).

Peptide MTM7 was produced on solid support using continuous flow chemistry by Pepceuticals Ltd., Leicester, UK. The final purity was tested by HPLC as well as mass spectrometry and was above 90%.

2.2. Solvents

Peptide MTM7 is a highly hydrophobic peptide with a poor solubility in DPC micelles, TFE:water mixtures, and aqueous systems. To perform conformational studies, two membrane-mimicking solvents commonly used in literature were selected: SDS micelles (SDS from Merck, Darmstadt, Germany and d_{25}-SDS from Cambridge Isotopes), and d_6-DMSO (Cambridge Isotopes) [18–20,22–24]. The natural properties of each solvent determine which spectroscopic technique can be used to study the conformational properties of peptide MTM7, as is discussed below. SDS-PAGE electrophoresis gels of peptide MTM7 dissolved in the solvents mentioned showed a single MTM7 band at 4.2 kDa, which indicates the absence of peptide aggregation.

2.3. Sample preparation

To prepare samples of peptide MTM7 solubilized in SDS for CD an NMR experiments, the peptide was initially dissolved in TFA and dried under a stream of nitrogen. A 3 mM solution was prepared in TFE resulting in a clear solution. This peptide solution was mixed with a freshly made SDS solution at the desired concentration. The final solution was clear. Deionized water was added to yield a volume ratio of 16:1. The sample was mixed for 15 min and rapidly frozen followed by drying under vacuum at −70°C. The dry samples were rehydrated with deionized water (pH 6.0) resulting in clear solutions [25]. The final peptide concentration was 2.0 mM. In all prepared SDS samples the concentration of SDS was well above the cmc. For the NMR samples d_{25}-SDS was used instead of unlabelled SDS.

2.4. CD measurements

Circular dichroism spectroscopy is a useful technique to determine the secondary structure of proteins and small peptides under various conditions [26–28]. Here, this technique could only be used to study the conformational behavior of peptide MTM7 in SDS micelles [18,20,22,24,27] because DMSO strongly absorbs below 240 nm, thereby prohibiting the extraction of secondary structure contents from CD spectra [27]. Sample preparation of peptide MTM7 in SDS micelles (peptide-to-SDS ratios were 1:100 and 1:250) was performed as described above. For each experiment freshly prepared sample was used. The concentration of peptide MTM7 was determined spectrophotometrically by measuring the UV absorbance at 280 nm, using an extinction coefficient of 12,740 l mol^{-1} cm^{-1} [29]. For all the experiments the O.D. was below 0.5.

Far-UV CD spectra were recorded on a Jasco J-715 spectropolarimeter, equipped with a Peltier thermal-controlled cuvette holder. The spectra were recorded using a 0.01 cm path length quartz cuvette, from 260 to 190 nm, with a 1.0 nm step resolution and a response time of 0.25 s. The spectra were collected and averaged over 25 scans. For the thermal stability experiments the ellipticity at 222 nm was measured between 20 and 50 °C, with a temperature interval of 1.0 °C. At each temperature the sample was allowed to equilibrate for 5 min. After reaching 50 °C the temperature was lowered again to 20 °C and a final spectrum was acquired to check for reversibility. All spectra were baseline corrected by using control samples without peptide.

The secondary structure content of peptide MTM7 was calculated using the method of Chen [30] and the CD spectra deconvolution software CDNN [31]. The CDNN software calculates the secondary structure content of a protein by comparison of its CD spectrum with a CD database of known protein structures. The method of Chen [30] assumes that the ellipticity at 222 nm is exclusively due to α-helix conformation. Thus the α-helix content of a protein $\{\alpha\}$ of n residues is given by [30]:

$$\{\alpha\} = \frac{[\theta]_{222}}{[\theta]_{222}^{\max}}\left(1 - \left(\frac{k}{n}\right)\right) \times 100, \quad (1)$$

where $[\theta]_{222}$ and $[\theta]_{222}^{\max}$ are the experimental and maximal (−39,500 deg cm^2 $dmol^{-1}$) values of the ellipticity at 222 nm, respectively. The wavelength dependent constant k is 2.57 at 222 nm.

2.5. NMR measurements

NMR samples were prepared in d_{25}-SDS at different peptide-to-SDS ratios (1:70, 1:100 and 1:250) as described above. For the NMR samples in DMSO, peptide MTM7 was dissolved in 500 μL of d_6-DMSO at a concentration of about 2 mM. Excess DTT (dithiothreitol) was added to the sample to avoid formation of disulphide bridges and peptide aggregation [32]. As an internal standard 0.1 mM DSS was used. ^{1}H NMR spectra were recorded at 750 MHz on a Bruker DRX750 spectrometer. Natural abundance 2D ^{1}H–^{13}C HSQC and HMBC spectra were recorded at 600 MHz on a Bruker spectrometer equipped with a cryoprobe. 2D NOESY and TOCSY spectra were recorded as described elsewhere [33]. All experiments were recorded at 30 °C. 2D NOESY experiments were acquired with mixing times of 100, 300 and 400 ms. 2D TOCSY experiments were acquired with a mixing time of 75 ms. In case of all 2D-NMR experiments 2K data points were collected in the t_2 dimension and 1K data points were collected in the t_1 dimension. The spectral width was 11 ppm for ^{1}H, 80 ppm for ^{13}C in the case of 2D ^{1}H–^{13}C HSQC and 160 ppm for ^{13}C in case of 2D ^{1}H–^{13}C HMBC. The NMR data were processed using XWINNMR from Bruker. Peak assignment and spectral analysis were carried out using NMRView [34] and Sparky (Goddard, T. D., and Kneller, D. G., University of California, San Francisco).

3. Results

3.1. Circular dichroism experiments

The far-UV CD spectra of peptide MTM7 in SDS micelles at peptide-to-SDS ratios of 1:100 and 1:250 are shown in Fig. 2. At both ratios the spectra show a maximum at 193 nm and two minima at 208 and 222 nm, respectively, suggesting the presence of helical structure in the peptide. The secondary structure analysis of the CD spectra of peptide MTM7 is compiled in Table 1. Both analysis methods are in good agreement: 21–22% helical content for a peptide-to-SDS ratio of 1:100 and 28–30% helical content for a peptide-to-SDS ratio of 1:250, respectively. For peptide MTM7 dissolved in TFE, the CDNN software indicates that is 100% α-helical, whereas the method of Chen leads to a helical content of 106%. The latter unrealistic percentage arises from the ellipticity value at 222 nm (−45,244 deg cm^2 $dmol^{-1}$) and is explained in Discussion. Both analysis methods show that MTM7 is in a full α-helical conformation in TFE. Indeed, TFE is known to induce the

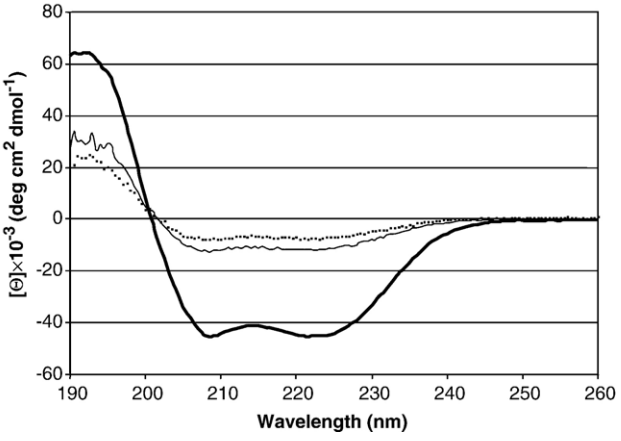

Fig. 2. Far-UV CD spectra of peptide MTM7 in TFE and in SDS micelles dissolved in deionized water (pH 6.0). MTM7 in TFE (▬), in 1:250 MTM7:SDS (–) and in 1:100 MTM7:SDS (▪▪▪). The final peptide concentration for all the samples is 2.0 mM. The temperature is 20 °C.

Table 1
Helical content of peptide MTM7 in SDS micelles as determined by Chen's method [30] and CDNN [31]

Sample	Chen's method (%)	CDNN (%)
Peptide to SDS ratio 1:100	21	22
Peptide to SDS ratio 1:250	30	28
TFE	106	100

The standard error in the percentage is approximately ±4%. The temperature is 20 °C.

formation and stabilization of helical regions in peptides and proteins that have an inherent propensity to do so [24,35].

We carried out CD experiments in peptide–SDS solutions at pH values from 2 to 12 in a 50 mM phosphate buffer. For both peptide-to-SDS ratios of 1:100 and 1:250, no changes were detected in the CD spectra (data not shown). We used high concentrations of peptide MTM7 in DMSO and SDS samples due to the technical demands to perform 2D NMR spectroscopy on a non-isotope labelled peptide. To ensure that no concentration effects were taking place, CD spectra were recorded at a 10 times lower peptide concentration, however, the spectra did not change.

To study the conformational stability of peptide MTM7, the ellipticity is measured at 222 nm as a function of temperature up to 50 °C (Fig. 3). At both peptide-to-SDS ratios the ellipticity changes with temperature in a linear way, but no defined unfolding transition is observed in the temperature range studied. Upon cooling of peptide MTM7 in SDS back to 20 °C, the ellipticity at 222 nm returns to its original value (Fig. 3). Thus, the unfolding behavior of peptide MTM7 has a low cooperativity and the conformational exchange between the helical and unfolded conformations of MTM7 is fully reversible.

3.2. NMR experiments in d_6-DMSO

2D NMR spectra of peptide MTM7 in d_{25}-SDS micelles with peptide-to-SDS ratios of 1:70, 1:100 and 1:250 contain

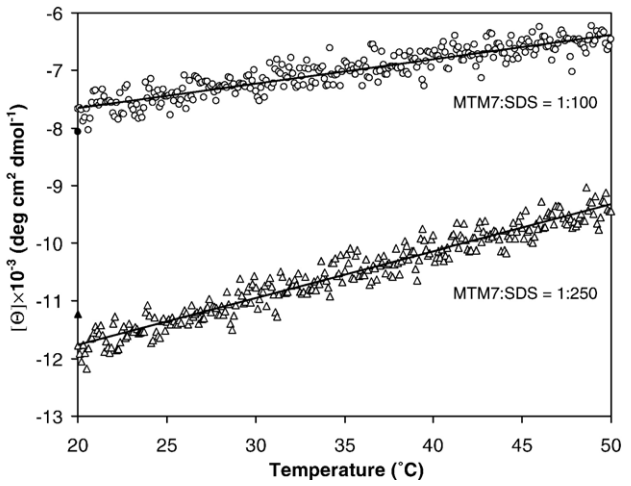

Fig. 3. Thermal stability experiment of peptide MTM7 solubilized in two different peptide-to-SDS ratios (1:250 and 1:100). The points ● and ▲ correspond to the CD measurements at 222 nm after cooling the sample to 20 °C.

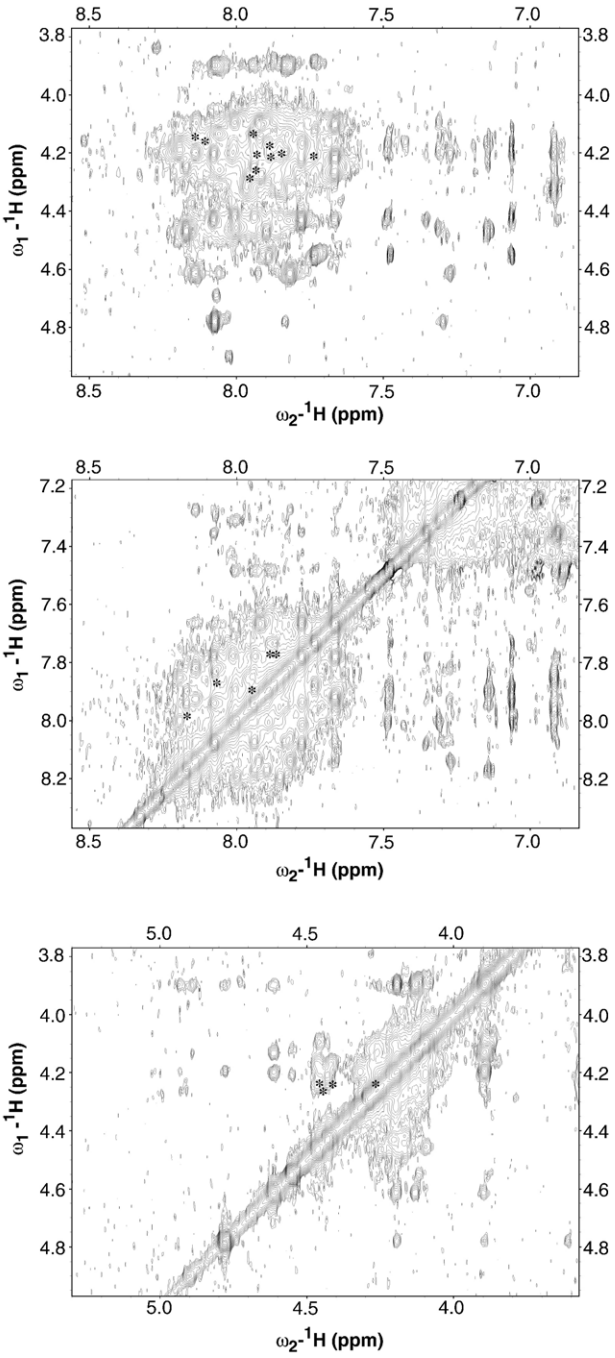

Fig. 4. Th^{1}H$_N$–^{1}H$_\alpha$ (top), ^{1}H$_N$–^{1}H$_N$ (middle) and ^{1}H$_\alpha$–^{1}H$_\alpha$ (bottom) regions of the 400 ms 2D NOESY spectrum of peptide MTM7 in d_6-DMSO. Broadening of cross peaks and resonance overlap limit the full assignment of all protons of MTM7. Broadening and overlapping regions are marked with an asterisk.

severely broadened cross peaks. As this effect is much less severe in d_6-DMSO, 2D ^{1}H–^{1}H TOCSY, NOESY and ^{1}H–^{13}C natural abundance HSQC and HMBC spectra of peptide MTM7 are recorded in d_6-DMSO. TOCSY, HSQC and HMBC spectra are used to identify the different spin systems. The $d_{NN}(i, i+1)$ NOE contacts observed in the NOESY spectra are used to sequentially assign the spin systems of peptide MTM7 [36,37]. Even in d_6-DMSO strong broadening and resonance overlap of some ^{1}H$_N$–^{1}Hα contacts prevents unambiguous assignment of

several spin systems (Fig. 4). The relatively large number of leucines, isoleucines and serines that have overlapping resonances further complicates resonance assignments. Despite these challenges 50% of the $^{1}H_N$ and $^{1}H\alpha$ resonances are assigned and are used for secondary structure analysis. The chemical shifts obtained for $^{1}H_N$, $^{1}H\alpha$ and $^{13}C\alpha$ are provided in Table 2 and are deposited in the BioMagResbank under access number BMRB-6878. This deposit also includes side chain proton assignments, the ^{13}C carbonyl, $^{13}C\alpha$ and $^{13}C\beta$ assignments). The $^{13}C\alpha$ chemical shift of 65.33 ppm found for A742 is unusual (Table 2). Currently, we do not have an explanation for this behavior.

The chemical shift index (CSI) method [38,39] is applied to the $^{1}H\alpha$ and $^{13}C\alpha$ resonances and the results are shown in Fig. 5. The combination of consecutive $^{1}H\alpha$ and $^{13}C\alpha$ CSI values indicates a propensity for an α-helix configuration for residues T730-A738 and A742-Q745. The helical propensity information for residues T730-A738 is limited due to the lack of assignments of several $^{1}H\alpha$ and $^{13}C\alpha$ nuclei (residues L734, L736 and L739 lack $^{1}H\alpha$ and $^{13}C\alpha$ assignments, and we were not able to assign S732), so no strong evidence of α-helical conformation can be concluded.

Table 2
$^{1}H_N$, $^{1}H_\alpha$ and $^{13}C_\alpha$ chemical shifts (in ppm) of peptide MTM7 dissolved in d_6-DMSO

Residue		$^{1}H_N$	$^{1}H_\alpha$	$^{13}C_\alpha$
717	I	—	—	—
718	H	—	—	—
719	T	8.07	4.23	60.00
720	I	—	—	—
721	E	—	—	—
722	F	8.08	4.47	62.06
723	C	—	—	—
724	L	—	—	—
725	N	7.90	4.59	56.32
726	C	—	—	—
727	V	7.94	4.25	—
728	S	—	—	—
729	H	8.14	4.65	61.64
730	T	7.81	4.17	—
731	A	8.17	4.28	56.80
732	S	—	—	—
733	Y	7.90	4.50	61.96
734	L	7.73	—	—
735	R	7.67	4.13	60.18
736	L	7.78	—	—
737	W	7.94	4.45	60.18
738	A	8.06	4.29	56.80
739	L	7.94	—	—
740	S	—	—	—
741	L	—	—	—
742	A	8.00	4.22	65.33
743	H	8.01	4.49	—
744	A	7.79	4.25	59.60
745	Q	8.20	4.21	66.60
746	L	—	—	—
747	S	—	—	—
748	S	—	—	—
749	V	7.76	—	—
750	L	8.12	4.54	57.90
751	W	—	—	—
752	T	7.72	4.16	61.80
753	M	—	—	—

A dash (—) indicates that no clear assignment was possible for this nucleus. These results are also published in the BioMagResbank under access number BMRB-6878.

In Fig. 5 also the $d\alpha_N(i, i+4)$ and $d\alpha_N(i, i+3)$ NOE contacts found for peptide MTM7 in DMSO are presented. These contacts provide another source that indicates whether a peptide segment has an α-helical conformation [36,37]. Combining the NOE contacts with the CSI data leads to the identification of three helical regions within MTM7: C723-A731, Y733-L739 and A742-V749 (Fig. 5).

4. Discussion

The putative seventh transmembrane segment of V-ATPase subunit *a* contains an arginine residue (R735), which is known to be essential for the function of V-ATPase. The exact role played by R735 is however still a matter of discussion. An interaction of R735 with the glutamic acid residue present in the fourth transmembrane segment of the rotor subunits *c*, *c′* and the second transmembrane segment from subunit *c″* has been suggested [3,7]. Unfortunately, no high-resolution structure of subunit *a* is available.

To overcome the typical problems associated with high-resolution NMR studies of transmembrane proteins [40] we designed peptide MTM7, which mimics the putative TM7 segment of subunit *a*, and investigated its conformational characteristics. Taking into account that TM7 is located in a proteic environment and is surrounded by other transmembrane segments of subunit *a* and by the transmembrane sections of the rotor subunits of V-ATPase, the peptide is expected to be highly hydrophobic. Indeed, at NMR concentrations (1 to 2 mM) peptide MTM7 is only soluble in the membrane-mimicking solvents used in this paper: SDS micelles and DMSO. The 2D-NMR spectra of peptide MTM7 in SDS micelles at different ratios show a low signal-to-noise ratio and a severe peak broadening, so no detailed conformational information could be extracted by NMR. Therefore the SDS micelle system was used to study the global conformation of the peptide by CD spectroscopy. As NMR broadening effects are much less severe in DMSO, this solvent was chosen to perform 2D-NMR experiments. Unfortunately, DMSO has a too high UV cutoff to permit the analysis of the peptide conformation by CD, so no direct comparison can be made with the CD results obtained in the SDS samples.

SDS is frequently used as a membrane mimetic environment in NMR and CD studies on transmembrane peptides and proteins [16,22,25,41–48]. CD spectroscopy in SDS micelles (Fig. 2) shows that peptide MTM7 has a tendency to adopt an α-helical conformation. The relatively low percentage of helical content of peptides and proteins dissolved in SDS micelles has been associated in literature to he use of SDS solutions below its CMC [26]. However in our work the concentration of SDS is always kept well above the typical CMC value of SDS. So for both peptide:SDS ratios studied the differences can be explained as follows. The hydrophobicity plot of peptide MTM7 shows that it has a positive hydrophobic index

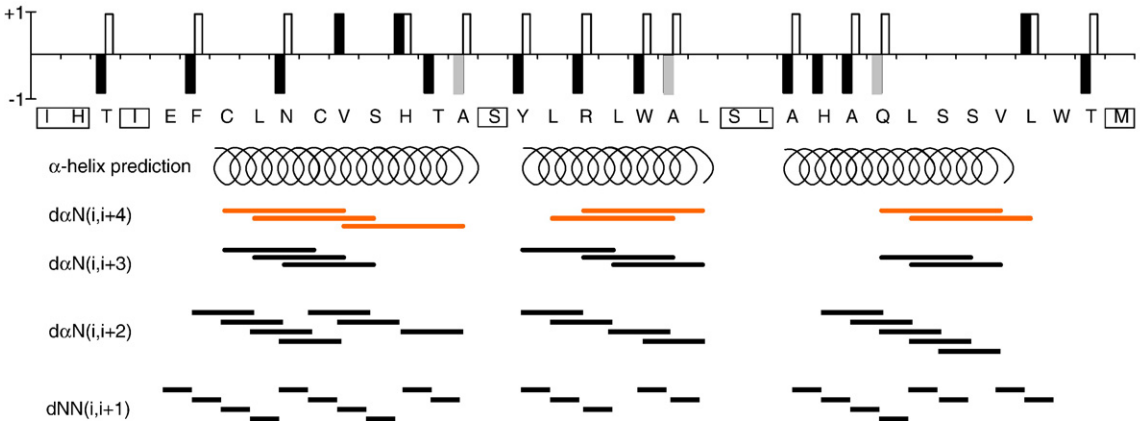

Fig. 5. Chemical shift index (■ - ^{1}Hα CSI; □ - ^{13}Cα CSI) [38,39] and NOE connectivities ($d\alpha_N(i, i+4)$, $d\alpha_N(i, i+3)$, $d\alpha_N(i, i+2)$, and $d_{NN}(i, i+1)$) of peptide MTM7 in d_6-DMSO. Gray CSI values represent residues with a ^{1}Hα CSI value indicative for a moderate tendency to form helices (Δδ(ppm) between −0.05 and −0.10). A consecutive appearance of CSI values of −1 for ^{1}Hα and +1 for ^{13}Cα indicate a propensity for an α-helix conformation. Such a sequence is found for residues T730-A738 and A742-Q745. For the residues T730-A738 the information is limited due to some missing assignments. Boxed residues have overlapping resonances and the resonance assignments are ambiguous. The predicted α-helical regions (▒) are based on the combination of CSI data and NOE connectivities.

extending from amino acid residue V727 to I757 (Fig. 6). Consequently, in a micellar environment like SDS, one would expect that the detergent molecules cover the C-terminal part of peptide MTM7 and that the N-terminal region of the peptide is exposed to the aqueous phase. Such a behavior has been found for other transmembrane peptides dissolved in similar micellar systems [22,41]. However, based on the analyses of the CD data peptide MTM7 has only a helical content between 21 and 30% for peptide:SDS ratios of 1:100 and 1:250, respectively. This low helical content can be explained in two ways: (1) the presence of the R735 in the middle of the peptide sequence might interfere with the peptide solubilization in the micelles [19]; (2) peptide MTM7 is expected to be relatively flexible, thereby rapidly undergoing multiple conformational states, which means that longer helices would break into smaller ones [28] and thus smaller ellipticity intensities would be obtained [49]. The low helical content calculated is due to the relatively low ellipticity values observed in the CD spectra, the other features of which are typically α-helical. This low ellipticity suggests that a relatively large fraction of the MTM7 molecules in the micellar systems dynamically populates the unfolded state (which has an almost zero CD intensity at 222 nm [28,50]).

CD spectroscopy shows that peptide MTM7 adopts an α-helical conformation in TFE (Table 1). The ellipticity minimum at 222 nm is −45,244 deg cm^2 dmol^{-1}. In addition to this anomalous value, the characteristic α-helical ellipticity maximum at 190 nm is red shifted to 193 nm. Both observations support that MTM7 contains a longer stretch of helical residues than commonly found in water-soluble globular proteins. Traditional secondary structure analysis packages are based on a comparison of the CD spectrum of interest with a library of CD spectra of water-soluble proteins. However in case of stretched transmembrane α-helical peptides it has been shown that the ellipticity at 222 nm can be more negative than −39,500 deg cm^2 dmol^{-1} and that the ellipticity maximum commonly found at 190 nm now exhibits a red shift [50]. From these results we assume that peptide MTM7 in TFE adopts a full α-helical structure possibly due to the natural propensity of the solvent used to induce such a structure. Due to this possible solvent artifact, we did not consider an NMR study of the peptide in TFE.

The difference in helical content of peptide MTM7 in SDS systems with peptide-to-SDS ratios of 1:100 and 1:250 can be attributed to the rather low solubility of peptide MTM7 in SDS micelles. At a peptide-to-SDS ratio of 1:100 the peptide is surrounded by a relatively low number of SDS molecules that cover the C-terminal part of MTM7 and provide a local hydrophobic environment in which the C-terminal part of the peptide dynamically populates an α-helical structure according to its α-helix propensity. The other part of the peptide, which is not surrounded by SDS molecules, is not in a favorable stabilizing environment, so it will be unfolded giving rise to no CD signal. Increasing the number of SDS molecules (1:250 sample) permits a new arrangement of the SDS molecules around the peptide and a larger part of peptide MTM7 will be covered by SDS [48]. As a result, a larger part of the peptide dynamically populates the helical state and thus a stronger CD signal at 222 nm is observed. Despite the low helical content detected due to solvent constraints, this result suggests a natural tendency of peptide MTM7 to adopt α-helical structure in the domains stabilized by the SDS molecules. The thermal unfolding results obtained for peptide MTM7 in SDS micelles indicate that its unfolding is reversible and has a low cooperativity (Fig. 3). Thus, MTM7 folding and unfolding is not a one-step process, but involves an ensemble of different intermediate structural states with similar free energies. The population of these states changes gradually upon increasing the temperature. Thus, the CD results in SDS micelles suggest that the peptide has an inherent propensity to adopt such a secondary structure in its highly hydrophobic natural environment in V-ATPase. However, no conclusive evidence can be obtained about which amino acid residues of MTM7 are involved in helix formation.

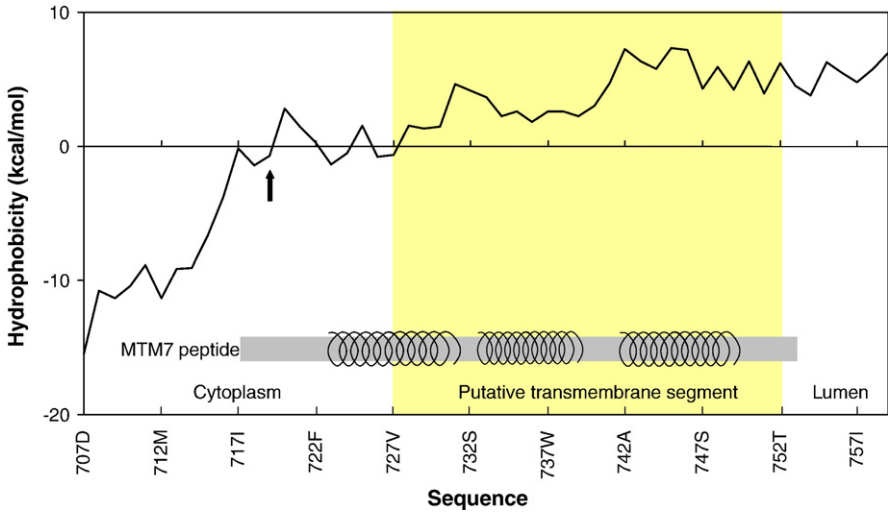

Fig. 6. Hydrophobicity plot of the region in which TM7 of V-ATPase from yeast is located. The hydrophobicity is calculated using the Mpex software (Jaysinghe, S., Hristova, K. and White, S. H. (2000) http://blanco.biomol.uci.edu/mpex). The putative TM7 region is marked in yellow and peptide MTM7 is shown by a gray bar. The three helical regions of peptide MTM7 as determined by NMR spectroscopy (Fig. 5) are depicted by ▒. The arrow indicates amino acid residue T719.

Although DMSO is known to have denaturing properties [51], experiments on different transmembrane proteins have shown that structures obtained in DMSO and DMSO–water mixtures accurately describe the structure of the protein or peptide in its native environment [23,52–54]. As peptide MTM7 is well soluble in DMSO in which it gives rise to reasonable quality NMR spectra (Fig. 4), we use DMSO as a solvent to study the conformation of peptide MTM7 by NMR spectroscopy. The combination of the CSI profiles and the NOE contacts indicates three α-helical regions in peptide MTM7: C723-A731, Y733-L739 and A742-V749 (Fig. 5). For the terminal sections of peptide MTM7 neither structural NOE contacts, nor consistent CSI (T719, L750 and T752) values are found. This is probably due to fraying of the terminal residues. For the two regions between the three helical sections no secondary structure information could be extracted from the NMR data due to cross peak overlap and/or severe cross peak broadening. Two CSI values are exceptional, the amino acid residues V727 and H729 have CSI values that could indicate the presence of a turn, or a helix bend around these residues. However, the CSI values should only be taken as a strong indicator of the helix propensity of the peptide; in fact, NOE contacts are a more reliable indicator of an α-helical conformation and they predict that V727 and H729 reside in a helical segment [36].

The hydrophobicity plot (Fig. 6) of the putative TM7 segment and of the adjacent putative loops, shows that the putative cytoplasmic loop has negative hydrophobicity values indicating that these residues are hydrophilic and located in the water phase. Starting with residue T719 the hydrophobicity values become positive for the first time, indicating that the subsequent section of the putative TM7 segment could be embedded in a hydrophobic environment. There are two small amphipathic oscillations that could indicate the region of TM7 located at the interface between the hydrophobic protein environment and the water phase cytoplasm. Nevertheless, from residue T719 to the luminal section, the average hydrophobicity increases and stays at a high level. Thus, instead of starting at V727 [9], the putative TM7 segment could already start at T719. On the luminal side of TM7 the hydrophobicity is high (Fig. 6) and this remains so in the segment beyond the putative TM7. The model for subunit *a* [3] indicates that TM7 connects to the next transmembrane segment (TM8) via a putative loop composed of 8 residues (from T752 to G760). Due to the high hydrophobicity of this loop, we assume that it will be located in a hydrophobic proteic region. In such a view, the TM7 tryptophan residue at position 751 could act as an anchor [55] in the interface between the hydrophobic protein environment and the water phase lumen.

The NMR results of peptide MTM7 in DMSO, combined with the CD data of the peptide in SDS micelles, indicate that the peptide has a high tendency to adopt an α-helical conformation in a hydrophobic environment. Peptide MTM7 in SDS micelles shows a tendency to increase its helical structure with an increase of SDS concentration (1:100 to 1:250). Nevertheless the SDS data show a lower helicity as compared to the NMR results, but they support the observations that peptide MTM7 has a propensity for α-helical conformation. Thus in its natural hydrophobic environment (i.e., subunit *a* from V-ATPase) the TM7 segment most likely is fully helical. This finding is in agreement with recent work from the group of Forgac [56]. In combination with the hydrophobic data discussed, we propose that the putative TM7 in subunit *a* is a 32-residue helical segment that spans from T719 (cytoplasmic side) to W751 (luminal side). However on basis of our data, it cannot be excluded that the helical segment contains small non-helical segments. The new putative TM7 segment is composed of 32 amino acid residues and is within a hydrophobic part of V-ATPase.

The proposed 32-residue helical seventh transmembrane segment can now be aligned and compared with its neighboring transmembrane subunits, especially with the transmembrane

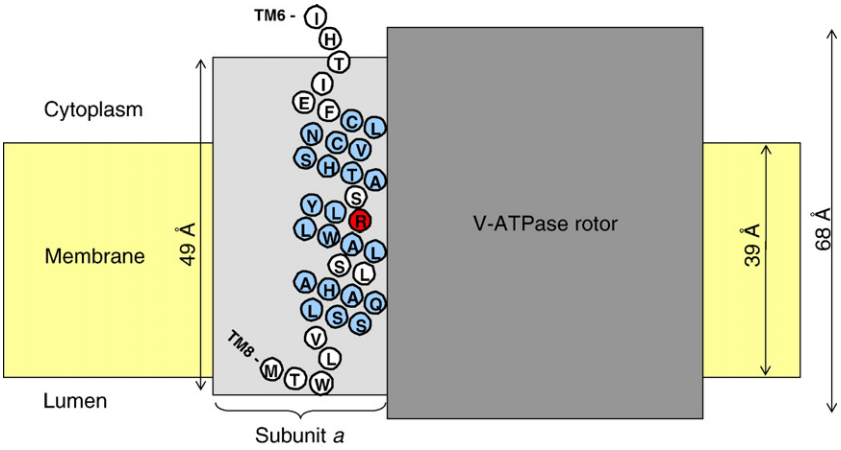

Fig. 7. Schematic representation of peptide MTM7 embedded in its natural environment (i.e. V-ATPase). The light gray box represents subunit *a*. The TM7 segment of subunit *a* runs from residue T719 up to W751 (see text). CD results show that TM7 is helical and this could be confirmed by NMR spectroscopy for the residues colored light blue. For the residues colored white no resonance assignment are available due to cross peak broadening and resonance overlap. The dark gray box represents the V-ATPase rotor and the yellow regions represent the membrane. Arginine residue 735 known to be involved in proton translocation is indicated in red. The height of the light gray box is calculated based on the demonstrated helicity of the comprising residues and assuming a rise of 1.5 Å per residue along the helical axis. The height of the rotor of yeast H^+-V-ATPase is based on the X-ray structure of the rotor subunit of Na^+-V-ATPase [7,57].

segments from the rotor subunits (*c*, *c*′ and *c*″) of V-ATPase. The 32-residue helix spans approximately 49 Å and we aligned the putative TM7 along the rotor subunit of V-ATPase (Fig. 7). TM7 needs to be in contact with the transmembrane segments present in subunits c, c′ and c″. This structural proximity is required as it forms the basis for the mechanism of proton translocation. This translocation occurs between R735 and the glutamic residues that are present in the subunit *c* assembly. The height of the rotor in the three-dimensional structure of the rotor subunits from F_1–F_O–ATPase from yeast [57] and Na^+-V-ATPase from *Enterococcus hirae* [7] is 58 and 68 Å, respectively. Besides the transmembrane helical segments it also comprises the cytoplasmic and luminal-embedded sections of the transmembrane rotor. The height of the rotor is thus larger than that of the proposed TM7. However, if one focuses on the localization and the length of the transmembrane sections of the rotor that interact with TM7, as determined for F_1–F_O–ATPase and Na^+-V-ATPase, some similarities are observed. The transmembrane segments found for F_1–F_O–ATPase are composed of 30 or 40 amino acid residues (depending on the segment involved) and are partially embedded in the cytoplasm. The four transmembrane segments present in the rotor of Na^+-V-ATPase include 28 to 35 amino acid residues and part of it is proposed to be embedded in the cytoplasm. The proposed TM7 of V-ATPase studied here comprises 32 amino acid residues (T719-W751), is helical and aligned along the rotor subunits. The length of a fully α-helical transmembrane section this long would be approximately 49 Å. Assuming that R735 is located in the middle of the membrane bilayer as it has to face the functionally important glutamic acid residues of the rotor subunits, and taking into account a bilayer thickness of 39 Å, TM7 extends into the cytoplasm with 9 of its residues and as this region is helical it has a height of approximately to 15 Å (Fig. 7). One side of this cytoplasmic part of TM7 interacts with the rotor of V-ATPase and in combination with the other transmembrane segments of subunit *a*. A small section of TM7 is positioned in the lumen and also interacts with the rotor of V-ATPase (Fig. 7). From a mechanistic point of view the proposed transmembrane localization of TM7 supports the current model that describes the action of V-ATPase. In this model, two hemi-channels emerge in which proton translocation occurs and the putative TM7 is supposed to be part of the cytoplasmic hemi-channel, where protons are transported into the membrane region.

In this paper we present, for the first time, experimental results that demonstrate that the seventh segment of subunit *a* adopts an α-helical structure. Based on the conformational results this segment adopts a more extended α-helical structure than predicted. In the new topology, TM7 spans from the lumen to the cytoplasm, where it is stabilized by a hydrophobic proteic environment (Fig. 7). This new topology will help to better understand the structure and function of subunit *a* in the H^+-V-ATPase enzyme.

Acknowledgments

This work was supported by contract no. QLG-CT-2000-01801 of the European Commission (MIVase-New Therapeutic Approaches to Osteoporosis: targeting the osteoclast V-ATPase). J.B.C.F. and M.A.H. are members of the COST D22 Action “Protein–Lipid Interactions” of the European Union. The NMR spectra were recorded at the SON NMR Large Scale Facility in Utrecht, which is funded by the “Access to Research Infrastructures” program of the European Union (HPRI-CT-2001-00172). We are indebted to Peter J. Meek for his bioinformatics contribution to the design of peptide MTM7.

References

[1] M.E. Finbow, M.A. Harrison, The vacuolar H^+-ATPase: a universal proton pump of eukaryotes, Biochem. J. 324 (1997) 697–712.
[2] M. Forgac, Structure, function and regulation of the vacuolar (H^+)-ATPases, FEBS Lett. 440 (1998) 258–263.

[3] T. Nishi, M. Forgac, The vacuolar (H^+)-ATPases—nature's most versatile proton pumps, Nat. Rev., Mol. Cell Biol. 3 (2002) 94–103.
[4] D. Chatterjee, M. Chakraborty, M. Leit, L. Neff, S. Jamsa-Kellokumpu, R. Fuchs, R. Baron, Sensitivity to vanadate and isoforms of subunits A and B distinguish the osteoclast proton pump from other vacuolar H^+ ATPases, Proc. Natl. Acad. Sci. U. S. A. 89 (1992) 6257–6261.
[5] Y. Arata, T. Nishi, S. Kawasaki Nishi, E. Shao, S. Wilkens, M. Forgac, Structure, subunit function and regulation of the coated vesicle and yeast vacuolar (H(+))-ATPases, Biochim. Biophys. Acta 1555 (2002) 71–74.
[6] M. Manolson, D. Proteau, R. Preston, A. Stenbit, B. Roberts, M. Hoyt, D. Preuss, J. Mulholland, D. Botstein, E. Jones, The Vph1 gene encodes a 95-kDa integral membrane polypeptide required for in vivo assembly and activity of the yeast vacuolar H^+-ATPase, J. Biol. Chem. 267 (1992) 14294–14303.
[7] T. Murata, I. Yamato, Y. Kakinuma, A.G.W. Leslie, J.E. Walker, Structure of the rotor of the V-type Na^+-ATPase from *Enterococcus hirae*, Science 308 (2005) 654–659.
[8] S. Wilkens, E. Vasilyeva, M. Forgac, Structure of the vacuolar ATPase by electron microscopy, J. Biol. Chem. 274 (1999) 31804–31810.
[9] S. Kawasaki-Nishi, M. Forgac, Proton translocation driven by ATP hydrolysis in V-ATPases, FEBS Lett. 555 (2003) 76–85.
[10] S. Kawasaki-Nishi, T. Nish, M. Forgac, Arg-735 of the 100-kDa subunit a of the yeast V-ATPase is essential for proton translocation, Proc. Natl. Acad. Sci. U. S. A. 98 (2001) 12397–12402.
[11] T. Nishi, S. Kawasaki-Nishi, M. Forgac, The first putative transmembrane segment of subunit c″ (Vma16p) of the yeast V-ATPase is not necessary for function, J. Biol. Chem. 278 (2003) 5821–5827.
[12] X.H. Leng, M.F. Manolson, Q. Liu, M. Forgac, Site-directed mutagenesis of the 100-kDa subunit (Vph1p) of the yeast vacuolar (H^+)-ATPase, J. Biol. Chem. 271 (1996) 22487–22493.
[13] S. Soulie, J.-M. Neumann, C. Berthomieu, J.V. Moller, M. le Maire, V. Forge, NMR conformational study of the sixth transmembrane segment of sarcoplasmic reticulum Ca^{2+}–ATPase, Biochemistry 38 (1999) 5813–5821.
[14] M.E. Girvin, V.K. Rastogi, F. Abildgaard, J.L. Markley, R.H. Fillingame, Solution structure of the transmembrane H^+-transporting subunit c of the F_1F_o ATP synthase, Biochemistry 37 (1998) 8817–8824.
[15] I. Ben-Efraim, Y. Shai, The structure and organization of synthetic putative membranous segments of ROMK1 channel in phospholipid membranes, Biophys. J. 72 (1997) 85–96.
[16] F. Li, H.Y. Li, L.H. Hu, M. Kwan, G.H. Chen, Q.Y. He, H.Z. Sun, Structure, assembly, and topology of the G185R mutant of the fourth transmembrane domain of divalent metal transporter, J. Am. Chem. Soc. 127 (2005) 1414–1423.
[17] V.Y. Orekhov, K.V. Pervushin, A.S. Arseniev, Backbone dynamics of (1–71) bacterioopsin studied by two-dimensional ^1H–^{15}N NMR spectroscopy, Eur. J. Biochem. 219 (1994) 887–896.
[18] M. Katragadda, J.L. Alderfer, P.L. Yeagle, Assembly of a polytopic membrane protein structure from the solution structures of overlapping peptide fragments of bacteriorhodopsin, Biophys. J. 81 (2001) 1029–1036.
[19] P.L. Yeagle, A.D. Albert, Use of NMR to study the three-dimensional structure of rhodopsin, Methods Enzymol. 343 (2002) 223–231.
[20] M. Adler, M.H. Seto, D.E. Nitecki, J.H. Lin, D.R. Light, J. Morser, The structure of a 19-residue fragment from the C-loop of the fourth epidermal growth factor-like domain of thrombomodulin, J. Biol. Chem. 270 (1995) 23366–23372.
[21] F.X. Ding, H. Xie, B. Arshava, J.M. Becker, F. Naider, ATR-FTIR study of the structure and orientation of transmembrane domains of the *Saccharomyces cerevisiae* alpha-mating factor receptor in phospholipids, Biochemistry 40 (2001) 8945–8954.
[22] G. Nielsen, A. Malmendal, A. Meissner, J.V. Moller, N.C. Nielsen, NMR studies of the fifth transmembrane segment of sarcoplasmic reticulum Ca^{2+}–ATPase reveals a hinge close to the Ca^{2+}-ligating residues, FEBS Lett. 544 (2003) 50–56.
[23] P.L. Yeagle, G. Choi, A.D. Albert, Studies on the structure of the G-protein-coupled receptor rhodopsin including the putative G-protein binding site in unactivated and activated forms, Biochemistry 40 (2001) 11932–11937.
[24] A. Jasanoff, A.L. Fersht, Quantitative determination of helical propensities from trifluoroethanol titration curves, Biochemistry 33 (1994) 2129–2135.
[25] J.A. Killian, T.P. Trouard, D.V. Greathouse, V. Chupin, G. Lindblom, A general method for the preparation of mixed micelles of hydrophobic peptides and sodium dodecyl sulphate, FEBS Lett. 348 (1994) 161–165.
[26] T. Lazarova, K.A. Brewin, K. Stoeber, C.R. Robinson, Characterization of peptides corresponding to the seven transmembrane domains of human adenosine A2a receptor, Biochemistry 43 (2004) 12945–12954.
[27] S.M. Kelly, T.J. Jess, N.C. Price, How to study proteins by circular dichroism, Biochim. Biophys. Acta 1751 (2005) 119–139.
[28] R.W. Hesselink, R.B.M. Koehorst, P.V. Nazarov, M.A. Hemminga, Membrane-bound peptides mimicking transmembrane Vph1p helix 7 of yeast V-ATPase: a spectroscopic and polarity mismatch study, Biochim. Biophys. Acta 1716 (2005) 137–145.
[29] S.C. Gill, P.H. von Hippel, Calculation of protein extinction coefficients from amino acid sequence data, Anal. Biochem. 182 (1989) 319–326.
[30] Y.H. Chen, J.T. Yang, H.M. Martinez, Determination of the secondary structures of proteins by circular dichroism and optical rotatory dispersion, Biochemistry 11 (1972) 4120–4131.
[31] G. Bohm, R. Muhr, R. Jaenicke, CDNN: quantitative analysis of protein far UV circular dichroism spectra by neural networks, Protein Eng. 5 (1992) 191–195.
[32] W.W. Cleland, Dithiothreitol, a new protective reagent for SH groups, Biochemistry 3 (1964) 480–482.
[33] J. Cavanagh, W.J. Fairbrother, A.G. Palmer III, N.J. Skelton, Protein NMR Spectroscopy. Principles and Practice, Academic Press, 1996.
[34] B.A. Johnson, R.A. Blevins, A computer program for the visualization and analysis of NMR data, J. Biomol. NMR 4 (1994) 603–614.
[35] F.D. Sonnichsen, J.E. van Eyk, R.S. Hodges, B.D. Sykes, Effect of TFE on protein secondary structure: an NMR and CD study using a synthetic actin peptide, Biochemistry 31 (1992) 8790–8798.
[36] K. Wüthrich, NMR in Biological Research: Peptides and Proteins, North-Holland/American Elsevier, Amsterdam, 1976.
[37] K. Wüthrich, NMR of Proteins and Nucleic Acids, Wiley, Amsterdam, NY, 1986.
[38] D.S. Wishart, B.D. Sykes, F.M. Richards, The chemical shift index—a fast and simple method for the assignment of protein secondary structure through NMR spectroscopy, Biochemistry 31 (1992) 1647–1651.
[39] D.S. Wishart, B.D. Sykes, Chemical shifts as a tools for structure determination, Methods Enzymol. 239 (1994) 363–392.
[40] J. Torres, T.J. Stevens, M. Samso, Membrane proteins: the 'Wild West' of structural biology, Trends Biochem. Sci. 28 (2003) 137–144.
[41] C.H.M. Papavoine, R.N.H. Konings, C.W. Hilbers, F.J.M. Van de Ven, Location of M13 coat protein in sodium dodecyl sulfate micelles as determined by NMR, Biochemistry 33 (1994) 12990–12997.
[42] C.H.M. Papavoine, J.M.A. Aelen, R.N.H. Konings, C.W. Hilbers, F.J.M. Van de Ven, NMR studies of the major coat protein of bacteriophage M13. Structural information of gVIIIp in dodecylphosphocholine micelles, Eur. J. Biochem. 232 (1995) 490–500.
[43] T.A. Cross, S.J. Opella, Hydrogen-1 and carbon-13 nuclear magnetic resonance of the aromatic residues of fd coat protein, Biochemistry 20 (1981) 290–297.
[44] G.D. Henry, J.D.J. O'Neil, J.H. Weiner, B.D. Sykes, Hydrogen exchange in the hydrophilic regions of detergent-solubilized M13 coat protein detected by carbon-13 nuclear magnetic resonance isotope shifts, Biophys. J. 49 (1986) 329–331.
[45] G.D. Henry, B.D. Sykes, Strategies for the use of NMR spectroscopy in biological macromolecules and assemblies, Bull. Can. Biochem. Soc. 24 (1987) 21–26.
[46] M. Lindberg, A. Graslund, The position of the cell penetrating peptide penetratin in SDS micelles determined by NMR, FEBS Lett. 497 (1) (2001) 39–44.
[47] K.V. Pervushin, A.S. Arsen'ev, A.T. Kozhich, V.T. Ivanov, Two-dimensional NMR study of the conformation of (34–65) bacterioopsin polypeptide in SDS micelles, J. Biomol. NMR 1 (1991) 313–322.
[48] M. le Maire, P. Champeil, J.V. Moller, Interaction of membrane proteins and lipids with solubilizing detergents, Biochim. Biophys. Acta 1508 (2000) 86–111.

[49] M.C. Manning, R.W. Woody, Theoretical CD studies of polypeptide helices: examination of important electronic and geometric factors, Biopolymers 31 (1991) 569–586.
[50] K. Park, A. Perczel, G.D. Fasman, Differentiation between transmembrane helixes and peripheral helixes by the deconvolution of circular dichroism spectra of membrane proteins, Protein Sci. 1 (1992) 1032–1049.
[51] M. Jackson, H.H. Mantsch, Beware of proteins in DMSO, Biochim. Biophys. Acta 1078 (1991) 231–235.
[52] P.L. Yeagle, C. Danis, G. Choi, J.L. Alderfer, A.D. Albert, Three dimensional structure of the seventh transmembrane helical domain of the G-protein receptor, rhodopsin, Mol. Vis. 27 (2000) 6125–6131.
[53] M. Bellanda, E. Peggion, R. Burgi, W. van Gunsteren, S. Mammi, Conformational study of an Aib-rich peptide in DMSO by NMR, J. Pept. Res. 57 (2001) 97–106.
[54] A. Motta, P.A. Temussi, E. Wunsch, G. Bovermann, A 1H NMR study of human calcitonin in solution, Biochemistry 30 (1991) 2364–2371.
[55] S. Mall, J.M. East, A.G. Lee, Transmembrane alpha helices, in: D.J. Benos, S.A. Simon (Eds.), Peptide–lipid Interactions, vol. 52, Academic Press, San Diego, 2002, pp. 339–370.
[56] Y. Wang, T. Inoue, M. Forgac, Subunit a of the yeast V-ATPase participates in binding of bafilomycin, J. Biol. Chem. 280 (2005) 40481–40488.
[57] D. Stock, A.G.W. Leslie, J.E. Walker, Molecular architecture of the rotary motor in ATP synthase, Science 286 (1999) 1700–1705.